Utilizing a novel quantitative interpretation workflow to derisk shallow hydrocarbon prospects — a Barents Sea case study

Laurent Olivier Feuilleaubois[1*], Valerie Charoing[1], Andrea Maioli[1] and Cyrille Reiser[1] demonstrate that combining separated wavefield imaging with high-resolution velocity computations improves the pre-stack amplitude analysis of shallow water hydrocarbon targets in the Barents Sea.

Introduction

Large areas of the Barents Sea, such as the formerly disputed zone between Norway and Russia in the eastern Barents, are still undrilled. An exploration licence was recently awarded over the Haapet Dome (PL859) to operators with a prime interest in shallow Jurassic reservoirs (Reiser et al., 2016). Multiple oil and gas discoveries made farther west, such as Goliat and Norvarg, make this part of the world a highly prospective area for hydrocarbons. Traditionally the combination of a hard seabed with relatively shallow water depths has prevented the recording of near offset reflection data for the shallowest sediments. It is therefore not surprising that the presence of shallow hydrocarbons in this area has only recently been revealed thanks to imaging techniques that use the energy from sea-surface reflections which provide the missing near angle information for reliable AVA analysis. This paper describes a regional rock physics study of the Barents Sea and a quantitative interpretation workflow using Separated Wavefield Imaging (SWIM) and Full Waveform Inversion (FWI) to identify leads over the Haapet Dome in absence of direct well information.

Shallow water depth and shallow reservoir targets lead to imaging challenges

The thick icecap that formed during the last glaciation over the Barents Sea started melting during the Late Pliocene, causing an isostasic anomaly, which led to a major uplift and erosion of up to 1500 m of sediments in the Haapet area (Henriksen et al., 2011). The current shallow water depth in the Barents Sea is a consequence of this regional uplift. Permian salt formed domes such as the Haapet Dome (Figure 1), causing further tectonic deformation and the lifting of Jurassic reservoirs as shallow as 200 m below the seabed in some locations. Rocks at the seabed exhibit very high velocities above 3000 m/s owing to their deeper burial history. The combination of high velocity sediments and the shallow water setting lead to a lack of small angle reflection data when efficient widespread acquisition templates are used, resulting in significant acquisition footprints (Rønholt et al., 2015). The absence of such near-angle reflection data makes precise AVA analysis of the recorded pre-stack data very challenging and unreliable.
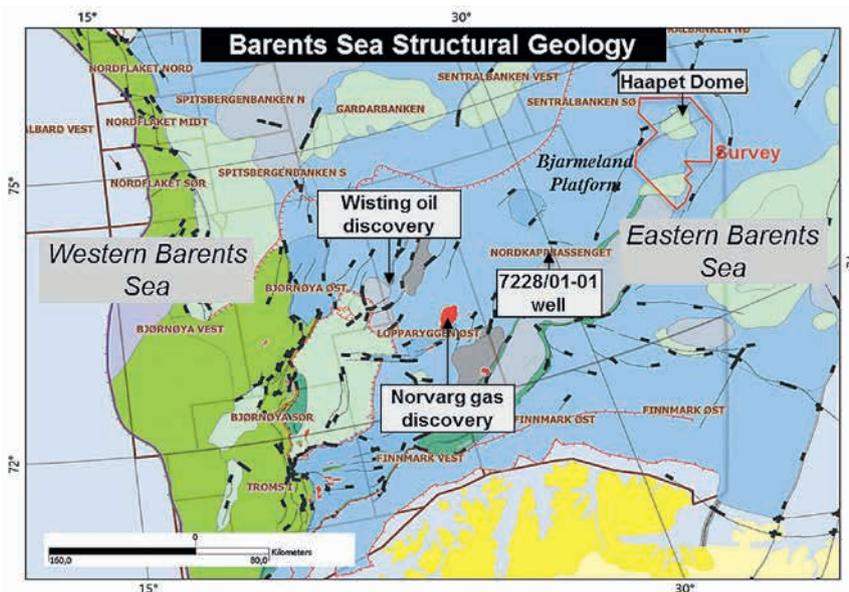

Figure 1 Structural map of the Barents Sea (Norwegian Petroleum Directorate).

[1] PGS

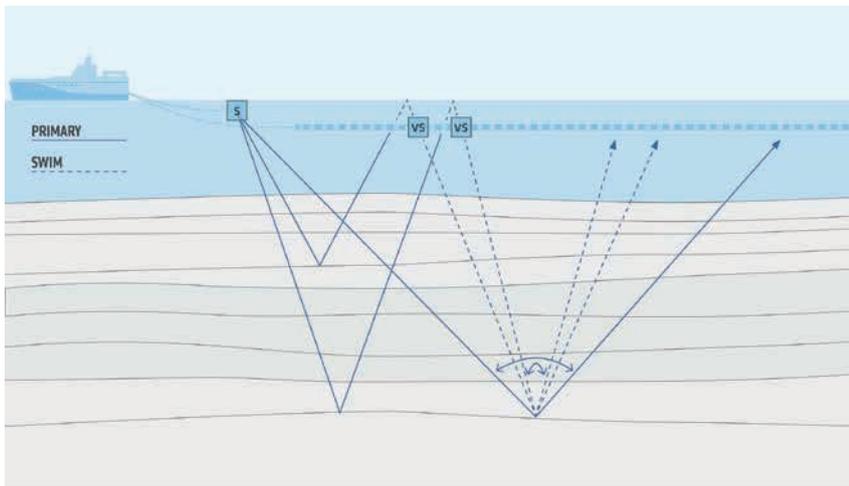* Corresponding author, E-mail: Laurent.Feuilleaubois@pgs.com

Figure 2 Separated Wavefield Imaging (SWIM) uses sea-surface reflections recorded by dual-sensor streamers to recover near-angle information even in very shallow settings with Source (S) and Virtual Source (VS).
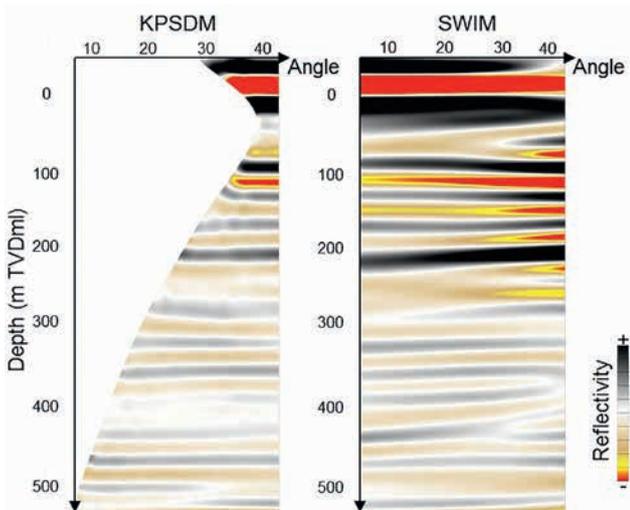

Figure 3 At the Jurassic target 250 m below the seabed K-PSDM (using primaries) delivers minimum recorded angles of 24 degrees whereas SWIM delivers near-angle traces down to 3 degrees by using sea-surface reflections.

Figure 4 Barents Sea South-East stratigraphic column based on an internal PGS study.

Acquisition and processing techniques focusing on shallow reservoir targets

Dual-sensor broadband 3D seismic surveys were acquired by PGS over the Haapet Dome on the Bjarmeland Platform in 2014 and 2015 (Figure 1). Two different processing methods were used, separated wavefield imaging and Kirchhoff pre-stack depth migration. Separated wavefield imaging (Whitmore et al., 2010) is a depth imaging technology that uses both up-going and down-going wavefields, recorded by the dual-sensor streamer system (Tenghamn et al., 2007). It effectively creates virtual sources at every receiver location in a marine seismic streamer spread which significantly enhances subsurface illumination and produces images of the seabed and shallow reflectors that primary reflections alone are not capable of (Ciotoli et al., 2016). This provides extended angular illumination of each point in the subsurface and recovers very near angles (Figure 2). This method also enables the reduction of seismic acquisition footprints and the widening of the lateral seismic coverage (Whitmore et al., 2010).

The minimum recorded angle was improved to 3 degrees using sea-surface reflections versus 24 degrees for primaries in the case of the Jurassic reservoirs in the Haapet survey area

(Figure 3). The wider angle range enhances shallow target AVA analysis by improving the statistical reliability of gradient and intercept volume computations. In combination with separated wavefield imaging and to improve the velocity analysis in a shallow environment, a refraction-based FWI has been performed to generate a high-frequency P-wave velocity model (Rønholt et al., 2015).

Kirchhoff pre-stack depth migration (K-PSDM) and SWIM angle gathers, as well as P-wave velocities derived from FWI, were conditioned for qualitative and quantitative interpretation. FWI was performed using frequencies up to 18 Hz. This enabled the generation of absolute pre-stack elastic attributes without the use of well information, as the FWI velocities filled the frequency gap between 0 Hz and the lowest seismic frequency

input into the inversion. The AVA-compliance of the SWIM data was assessed and verified against the K-PSDM data before the FWI integration into the pre-stack seismic inversion. Lithology and AVA class maps extracted from relative and absolute elastic pre-stack attributes were generated to identify potential leads on the topographic high formed by the Haapet Dome.

Jurassic reservoir geology

The main clastic reservoirs in this part of the world are Triassic (Snadd and Kobbe formations) and Jurassic (Stø, Nordmela and Tubåen formations) deposited throughout the Barents Sea from the Mid Triassic to Mid Jurassic (Figure 4). The sands, which originated from the erosion of the newly formed Ural Mountains, were mainly deposited in coastal environments switching between fluvial plains and shoreface (Smelror et al., 2009) followed by a major transgression, at the end of the Late Jurassic. The porosity in the Jurassic sandstones usually reaches 20% with a permeability of 700mD (e.g. Snøhvit area). Lack of well data in a radius of 250 km around the PL859 block, means that no well tie could be performed to pick the different formation tops on the seismic data. The Stø, Nordmela and Tubåen formations were therefore grouped in order to simplify

the interpretation and will be referred to from now on as Stø/Tubåen sandstones.

Maximum sea level was reached by the beginning of the Cretaceous period with the deposition of the Hekkingen organic-rich shale, which forms a regional marker. The lateral equivalent is the Kimmeridge clay in the North Sea. A hiatus is shown in the stratigraphic column, where the Cenozoic and most of the Cretaceous units were eroded owing to the post-glacial uplift (Smelror et al., 2009). Despite the current shallow burial depth as a result of this uplift, maturity of the Permian and potentially Lower Triassic source rocks is expected in the Haapet area. However, the Hekkingen shale is only expected to be mature in the south-western part of the Nordkapp Basin (Figure 5).

Regional rock physics and AVA modelling

Owing to post-glacial rebound during the late Neogene, a large regional uplift occurred reaching 3000 m in the Stapen High. It is possible to estimate and map the amount of uplift and erosion across the Barents Sea (Figure 6a) using various techniques. Mapping the Opal A/CT boundary (sometimes visible on seismic data) can be used along with geochemical analysis of well data such as the vitrinite reflectance index or the
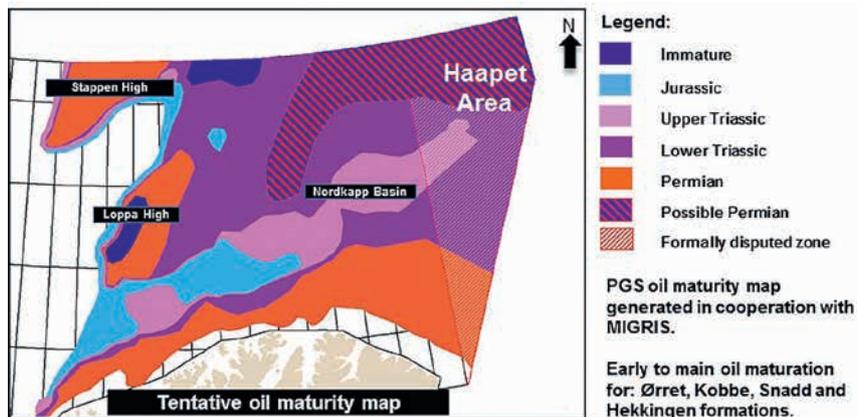

Figure 5 Maturation map of the Barents Sea showing the youngest source rock estimated to be mature (PGS internal study).
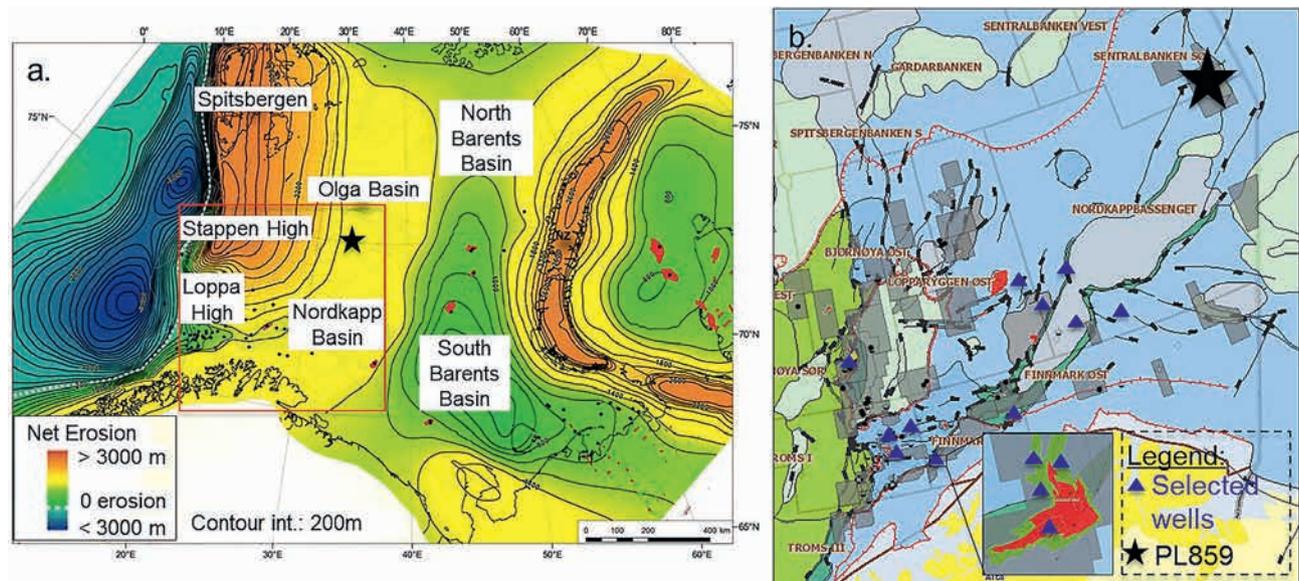

Figure 6 A regional map illustrating the estimated net erosion for the Greater Barents Sea from Henriksen et al., 2011. b Locations of a selection of 13 wells across the Barents Sea to provide data on Jurassic and Triassic reservoirs in various uplift regimes.
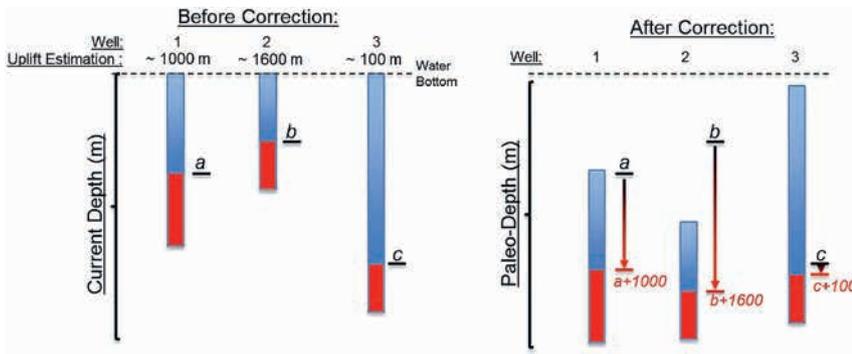
Figure 7 Correction for uplift is applied to each well using Henriksen's uplift and erosion map. The depth axis shows thereafter the paleo-depth before uplift or maximum burial depth.

Figure 8 Rock physics depth dependant trends derived using end member picking at maximum depth of burial for brine reservoirs.
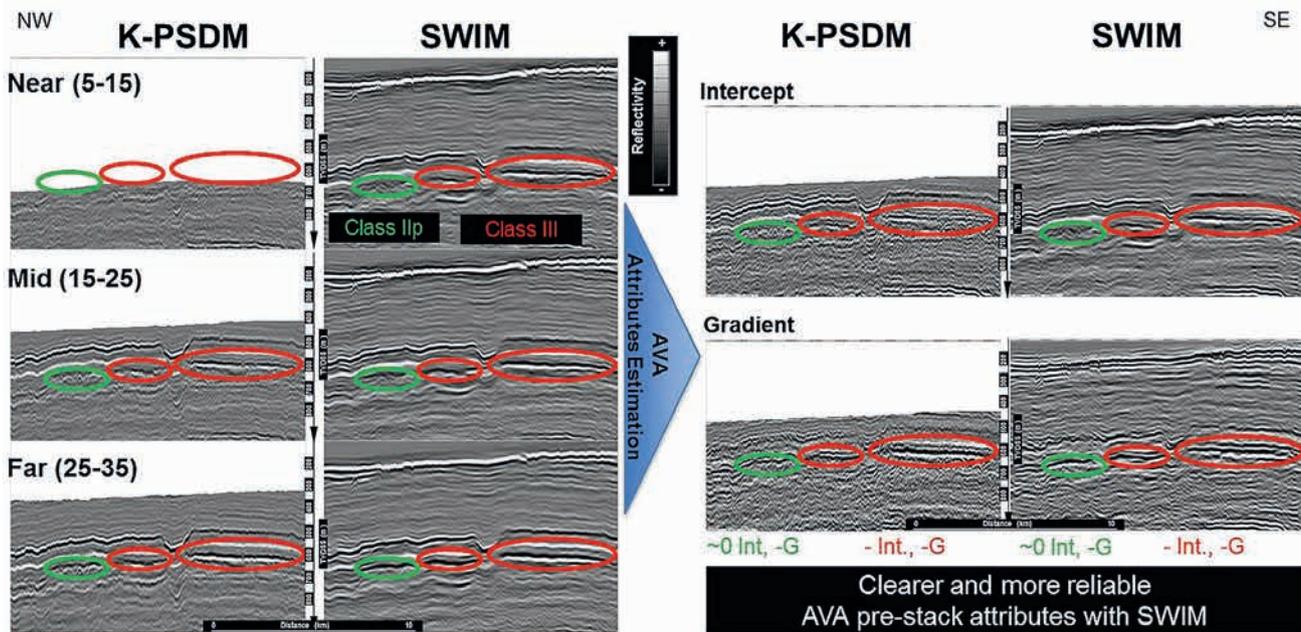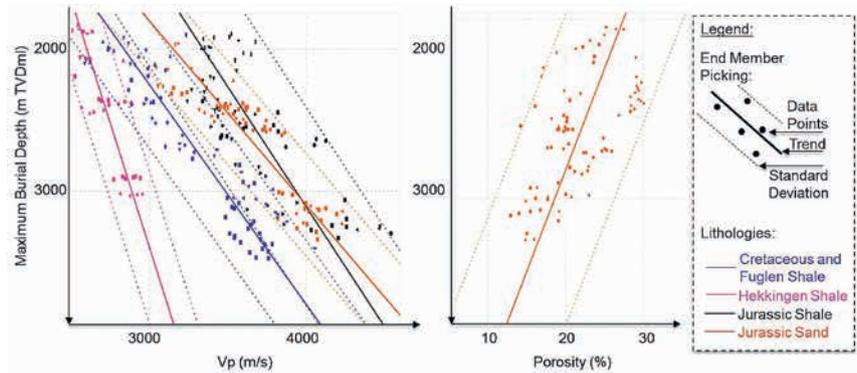

Figure 9 Comparison between K-PSDM and SWIM datasets through intercept/gradient (Shuey 2-Term equation). Similar AVA signatures (Class IIp in green and Class III in red) are observed and more stable attributes are estimated using separated wavefield imaging.

shale compaction trend from sonic logs and compared to seismic velocities (Henriksen et al., 2011). These geophysical and geochemical markers record the pressure and temperature reached at the maximum paleo-burial depth. Most of the uplift and erosion is believed to have taken place over the past three million years (Fjeldskaar et al., 2013). Based on a fast and very recent uplift, it is assumed that no major low pressure and low temperature metamorphism has occurred since, and that the rock properties therefore have remained the same as they were at the deepest burial depth.

Rock physics analysis can help to assess the prospectivity potential in frontier areas such as the remote Haapet area which is located 250 km from the closest exploration well, 7228/1-1. Identifying clear regional compaction trends and the relationships between rock physics properties for each lithology are key to modelling the potential response of a reservoir in such a remote location. Fourteen wells were selected from various uplift regimes in the Barents Sea including discoveries such as Snøhvit, Wisting, Johan Castberg and Goliat (Figure 6b). Hydrocarbon-bearing reservoirs were subsequently fluid substituted with brine

properties using Gassmann's equations. Fluid properties were extracted from the Norvarg discovery for gas, the Wisting discovery for oil and the 7228/1-1 dry hole for brine.

The variable uplifts across the area make a regional reservoir characterization approach very challenging. A sandstone deposited over a large area and then buried may lie today at variable depths totally unrelated to its maximum burial depth. To compare the physical properties of these two sandstones today, a simple workflow based on Henriksen's work was created. Using an uplift and erosion map (Henriksen et al., 2011), each well was corrected for the amount of uplift estimated to have occurred locally (Figure 7).

By doing so, a paleo-regional rock physics model using an end-member picking technique was generated. This method consists of picking the cleanest members of sandstones and shale in each well at various depths in order to identify depth dependant trends in the rock physics properties (Figure 8).

P-velocity, S-velocity, porosity and density paleo-trends prior to the Late Neogene were generated using end member picking. The deep marine shales, such as the Cretaceous and Jurassic Fuglen shales, plot on the same compaction trend whereas the rest of the Jurassic shales behave differently. The shales were

therefore split into two different groups. The Hekkingen shale was treated separately owing to significantly different properties related to its rich organic content. Figure 8 also shows that most of the Jurassic sandstones in the Barents Sea have a porosity greater than 20%.

Today in the Haapet area, the Jurassic reservoirs lie, on average, at 300 m below seabed. The level of uplift affecting this zone is estimated at 1500 m according to Henriksen's work (Figure 6a). Therefore, a simple calculation suggests that these Jurassic reservoirs were buried at 1800 m below the paleo-seabed before the Late Neogene. According to these results, an average porosity of 25% could be expected in the Jurassic in the Haapet area (Figure 8).

AVA compatibility of SWIM with K-PSDM dataset

Using only primary reflection seismic energy and Kirchhoff migration (K-PSDM), the targeted Jurassic reservoir interval lying at 300 m below seabed is not imaged on the near-angle stack (10 degree average angle). The wider angle range provided by SWIM helps to estimate more stable intercept and gradient attributes at the target and up to the seabed (Figure 9).
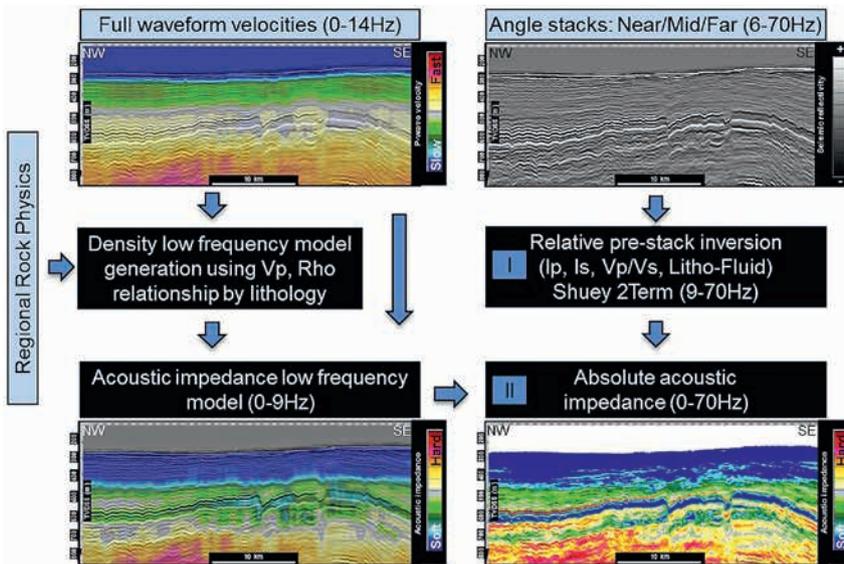

Figure 10 Quantitative interpretation workflows integrating separated wavefield seismic data and FWI P-velocities for reservoir characterization in areas with limited access to well information.
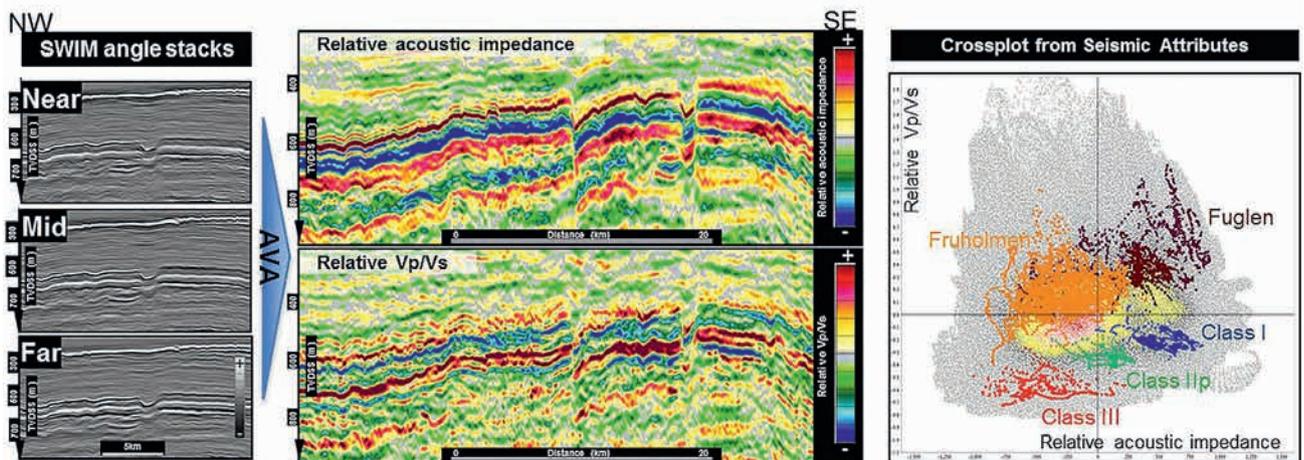

Figure 11 Relative Ip and relative Vp/Vs estimation using separated wavefield imaging pre-stack information leading to lithology and AVA class detection.

A clear negative gradient is observed on both separated wavefield and K-PSDM datasets at the top Stø/Tubåen reservoir (Figure 9). Both datasets also show, along this negative event, an intercept varying from zero (green circles) to negative (red circles) which could indicate a different fluid fill. Thus, there are some strong similarities in AVA response between the two datasets, indicating compatible AVA behaviours between SWIM and K-PSDM. This demonstrates that separated wavefield imaging is an AVA-compliant approach and it can be used as an input for quantitative interpretation work.

Quantitative interpretation workflows

Two different pre-stack quantitative analysis workflows were implemented. Firstly, only separated wavefield pre-stack seismic information was used to generate relative elastic attributes (Figure 10). Secondly, the high frequency FWI P-velocities (0-14 Hz) were converted to a low frequency acoustic impedance model volume (absolute) before being integrated to the relative elastic product and used to generate an absolute acoustic impedance volume (Figure 10).

Reservoir characterization using relative pre-stack attributes

Relative acoustic (Ip) and shear impedance (Is) volumes were generated from three angle stacks (near 5-15, mid 15-25 and far 25-35) before creating a relative velocity ratio (Vp/Vs) volume (Figure 11). The relative shear impedance was scaled to the relative acoustic impedance using the linear relationship between Vp and Vs derived from the regional rock physics.

A relative acoustic impedance versus relative velocity ratio (Vp/Vs) cross plot helps to identify the main stratigraphic units in relation to the rock physics study: Fuglen, Stø/Tubåen, and Fruholmen formations (Figure 11). The three AVA classes, highlighted on the cross plots, are observed at the top of the Stø/Tubåen reservoir and are respectively Class I, IIp and III. In order to enhance the existing discrimination between lithology cases and AVA classes, axis rotations in relative acoustic impedance versus relative Vp/Vs were performed to enhance sand predictions and AVA class recognition (Figure 12). Top and bottom Stø/Tubåen sandstones were then interpreted to estimate the potential thickness of the reservoir (Figure 14). Consistent AVA signatures are observed across fault blocks, which indicate a possible permeable connection between blocks (Figure 12). A normal sealing fault seems to limit the extension of the reservoir towards the south east, where only Class I sandstones are interpreted.

Integrating FWI P-Velocities without direct well data

In order to further understand the reservoir, an absolute acoustic impedance volume was generated. In the absence of any direct well data in the Haapet area, a low frequency model had to be built to fill the missing frequencies of the relative pre-stack acoustic impedance down to 0 Hz. The FWI P-velocities were converted to impedance, guided by geological horizons, and using the relationship derived from the regional rock physics study. Below the top Stø/Tubåen formation, the relationship for brine sand was applied everywhere to avoid biasing the density model towards the response of hydrocarbon filled sandstones.
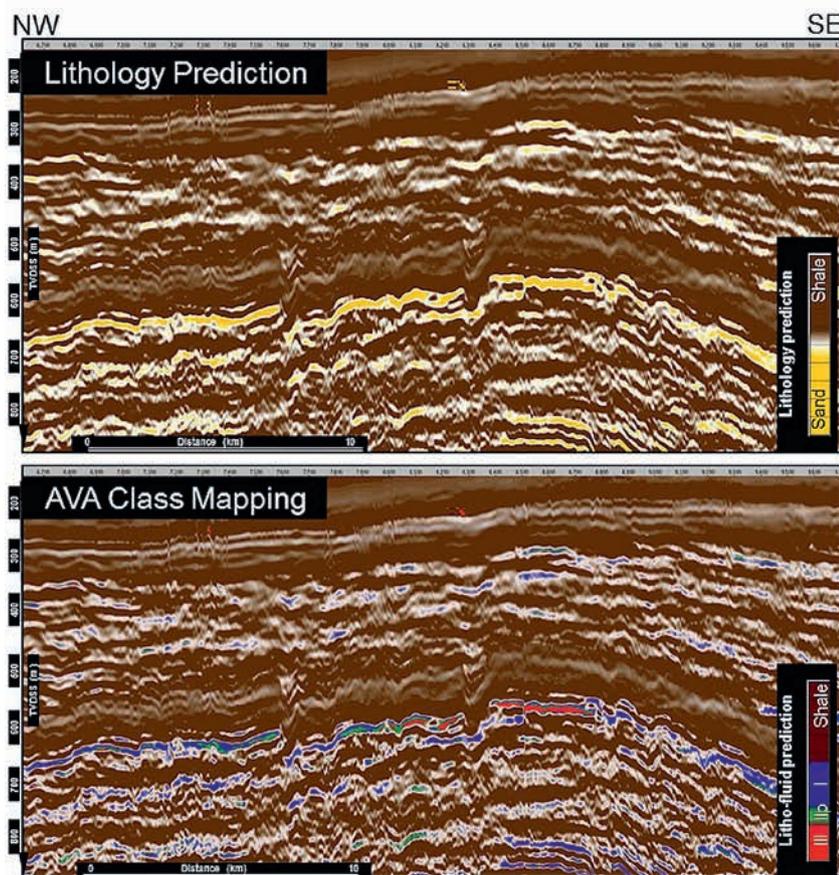

Figure 12 Lithology classification and AVA class mapping using AVA rotations in the relative Ip versus relative Vp/Vs domain.
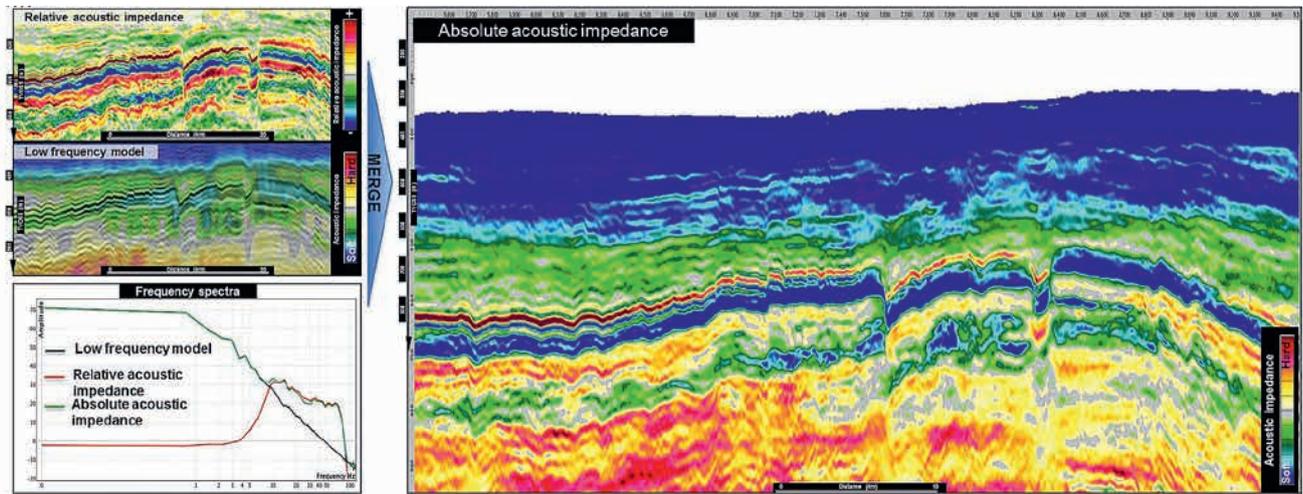
Figure 13 Absolute acoustic impedance obtained by merging scaled relative acoustic impedance with an acoustic impedance low frequency model derived from FWI.
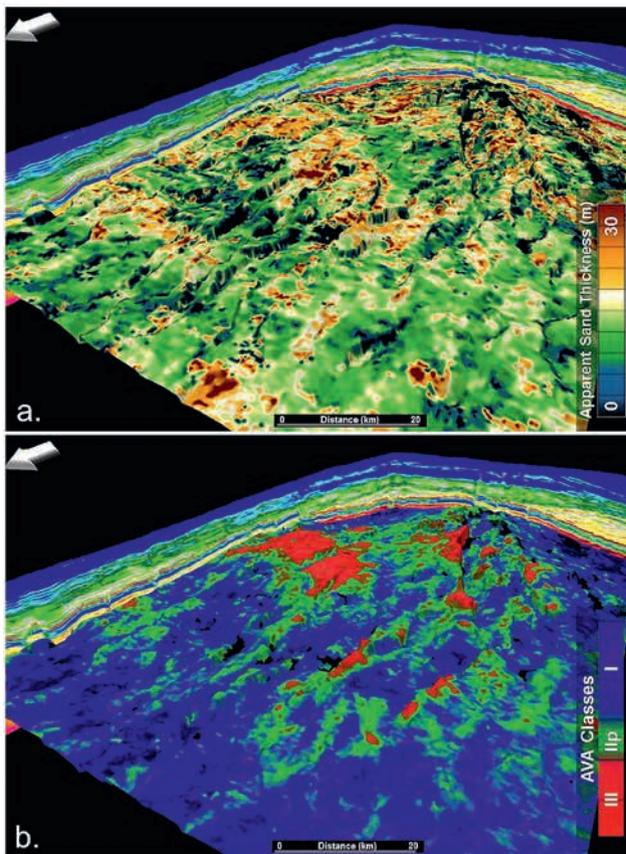

Figure 14 a 3D maps of apparent Stø/Tubåen sand thickness based on AVA rotation b. AVA class mapping using cut-offs on the absolute acoustic impedance volume.

The FWI P-impedance volume was then low-passed at 9 Hz (Figure 13). The low frequency model is then merged at 9 Hz with the estimated scaled relative acoustic impedance present from 9 to 70 Hz (Figure 13). To scale the relative acoustic impedance, the reflectivity coefficient at the Base Cretaceous Unconformity was scaled to the well 7228/1-1, estimated to have a consistent maximum burial depth with the Haapet area (Henriksen et al., 2011).

Quantitative analysis and prospectivity

Figure 14 shows the top Stø/Tubåen Formation covering an area of 2000 km². The thickness of the reservoir (Figure 14a)

was estimated using relative AVA rotated attributes as discussed earlier in the relative workflow. The sand reservoir seems to be continuous throughout the whole Haapet area and its thickness can reach 30 m locally. The tuning thickness of these sandstones was estimated to be around 9 m (based on modelling) and, gives a good degree of confidence when it comes to resolution of the thick reservoirs. Due to destructive interference near the top reservoir, it is possible that, below 9 m, the reservoir thickness is overestimated but sand should still be present. Based on the extent of the deposit and the absence of channelized features, the depositional environment seems be of a large scale and high energy similar to an estuary or a coastal margin. These types of depositional environments are usually associated with well sorted and clean sandstones and unlock the potential for high-quality reservoirs as suggested by the regional rock physics model which supports porosity levels above 20%.

Simple colour-coded cut-offs on the absolute acoustic impedance were created to reproduce the different AVA signatures observed at top Stø/Tubåen as previously shown on the relative Ip versus relative Vp/Vs cross-plot: Class I, IIp and III (Figure 11). This colour code was then used to map in 3D the average acoustic impedance between the top and base Stø/Tubåen reservoir (Figure 14b). Multiple Class III responses comprising two very large and other smaller anomalies stand out and seem to fill up the topographic highs. Class IIp responses appear in association with them and are conformable with the structures. Outside these closures, the anomalies disappear and a Class I response is mapped. It is very likely that these variations in AVA signatures that are present in acoustic impedance are linked to the presence of current or paleo-fluid fills. The first exploration well in the PL859 licence is planned for summer 2017 and will hopefully address this uncertainty.

Conclusion

In frontier areas, where well control is sparse, using all available seismic information is essential in identifying leads and de-risking prospects. The case study presented here, illustrates how the newly developed separated wavefield imaging technique is as AVA-compliant as Kirchhoff pre-stack depth imaging and improves the pre-stack amplitude analysis in the shallow

water context as discussed here. It also demonstrates that imaging using separated wavefields can be used for qualitative and quantitative interpretation in areas where the reservoir is just a few hundred metres below the seabed. FWI data were integrated into a quantitative interpretation workflow which helped to generate absolute elastic attributes and further de-risk prospects in the absence of local well information. Finally, the regional rock physics approach of the shallow Jurassic reservoirs in the Barents Sea seems to indicate very high potential for prospectivity with porosities above 20%. The presence of three different AVA signatures, conformable to topographic structures suggests the presence of more than one fluid but a risk linked to biodegradation remains. The first exploration well will be drilled in the Korpfjell prospect during the summer 2017 in the PL859 block and will remove this uncertainty. Further work over the Haapet area suggests porosity above 12% in the deeper section at the Triassic level. These findings open up the possibility of a new hydrocarbon play and in turn make this part of the Barents Sea one of the most exciting exploration targets in Europe.

Acknowledgements

References

Ciotoli, M., Beaumont, S., Oukili1, J., Korsmo, Ø., O'Dowd, N., Rønholt, G. & Dirks, V. [2016] Dual-sensor data and enhanced depth imaging sheds new light onto the mature Viking Graben area. *First Break* volume 34, pp. 73-79.

Fjeldskaar, W. & Amantov, A. [2013] Neogene Uplift of the Barents Sea. FORCE seminar, Tectonor/UiS, Stavanger, Norway.

Rønholt, G., Korsmo, Ø., Naumann, S., Marinets, S., Brenne, E. & Abbasi, M., F. [2015] Complete wavefield imaging for lithology and fluid prediction in the Barents Sea Grunde. SEG Annual Meeting New Orleans, Extended Abstract.

Henriksen, E., Bjørnseth, H. M., Hals, K. T., Heide, T., Kiryukhina, T., Kløvjan, O. S., Larssen, G. B., Ryseth, A. E., Rønning, K., Sollid, K. & Stoupakova, A. [2011] Uplift and erosion of the greater Barents Sea: impact on prospectivity and petroleum systems. Geological Society, London. *Memoirs*, 35, pp. 217–281.

Reiser, C. & Bird, T. [2016] Advances in broadband quantitative interpretation. SEG Annual Meeting Dallas, Extended Abstract.

Smelror, M., Petrov, O., Larssen, G. B. & Werner, S. C. [2009] *ATLAS – Geological history of the Barents Sea*. Norges geologiske undersøkelse.

Tenghamn, R., Vaage, S., and Borresen, C. [2007] A dual-sensor towed marine streamer; its viable implementation and initial results, 77th Annual International Meeting, SEG, Extended Abstract.

Whitmore, N. D., Valenciano, A.A., Sollner, W. and Shaoping, L. [2010] Imaging of primaries and multiples using a dual-sensor towed streamer, Exposition and 80th Annual Meeting. SEG Annual Meeting Denver, Extended Abstract.

ADVERTISEMENT